



Application of Satellite Remote Sensing on the Tuna Fishery of Eastern Tropical Pacific

Cho-Teng Liu and Ching-Hsi Nan
Institute of Oceanography, National Taiwan University, Taiwan, ROC
ctliau@ntu.edu.tw

Chung-Ru Ho, Nan-Jung Kuo and Ming-Kuang Hsu
Dept. of Oceanography, National Taiwan Ocean University, Taiwan, ROC

Ruo-Shan Tseng
Dept. of Marine Resources, National Sun Yat-sen University, Taiwan, ROC

Abstract. Tuna fishery is a major fishery in Taiwan, as in many other countries. Most of the tuna studies were based on the fish catch data, and their main subjects are related to the maximum sustainable yield of tuna. Both in managing the tuna fishery by the authorities (to maintain the size of standing stock), and in maximizing the catch per unit effort (CPUE) by fishing boats, one must know what are preferred oceanographic conditions to tuna. After analyzing tuna catch data from a few experimental fishing boats in the eastern tropical Pacific Ocean, we reached the following conclusion: (1) For predicting the fishing ground of tuna, using the mean distribution of sea surface temperature (SST) or ocean color is not better than making no-prediction, i.e. using the mean distribution of tuna catch. (2) CPUE of Big Eye tuna is higher in regions of SST in 26°C~28°C, surface Chlorophyll a concentration around 0.2 mg/m³, surface current speed above 0.15 m/s, or higher sea surface height (SSH). Because all the marine environmental parameters may change quickly with time or in space, satellite remote sensing data can provide the near real time observation for timely predictions of tuna fishing ground in the vast ocean.

Keywords: satellite, remote sensing, tuna, Pacific

1 Introduction

Tuna is a fast swimming fish that migrates thousands of miles. In the case of western North Pacific, the size of landed tuna increases along Kuroshio, but the landed tuna east of Mindanao has bi-modal structure, the juvenile and the matured tuna. To close its cycle of migration or its life

cycle, we may assume that the water near Mindanao may be the breeding ground of tuna that swims along Kuroshio for thousands of kilometers.

Long migration path may be a common character of tuna in all oceans. But, few tuna were tracked for studying its life history. Most tuna studies were based on catch data that were reported to the fishery administrations. The catch data on juvenile tuna were not recorded by the commercial fishing boat because they are not marketable. From the catch statistics published by the Food and Agriculture Organization of United Nations, the eastern tropical Pacific (ETP) is a region of high tuna catch since 1962. In this region, there are five major ocean currents, South Equatorial Current, Equatorial Counter Current, North Equatorial Current, Equatorial Under Current, and the weak South Equatorial Counter Current. The 5°x5° averaged, annual mean catch statistics (Fig. 1) is likely an average over three current systems, and therefore can hardly provide any information on the correlation between the marine environment and the fish catch.

If tuna has their preferred living environment, like all other animals, then the fish catch statistics should have some correlation with the marine environmental parameters, like surface temperature (SST), surface Chl. a concentration that is highly related to the primary productivity, ocean current, eddy, mixed layer depth, the thermocline depth, vertical temperature distribution, sea states, water clarity, etc.. For example, Taiwanese spear fishermen prefers high seas to catch tuna, instead of a sunny day with calm seas. For the far sea tuna fishermen, SST is still their primary factor in selecting fishing ground.

2 Oceanographic and Fish Catch Data

The water temperature data used in this study are the weekly mean SST from IGOSS (Integrated Global Ocean Services System), the temperature profile data are from NODC (National Oceanographic Data Center) for estimating the

mean temperature drop from surface to 100 m and to 200 m depth, the tuna catch data are from (1) IATTC (Inter-America Tropical Tuna Commission) for the 5°x5° averaged, monthly mean catch statistics, and (2) experimental fishing boats that was sponsored by the Fishery Administration (FA) of ROC. The satellite-derived Chl. a concentration is from SeaWiFS data bank of US NASA.

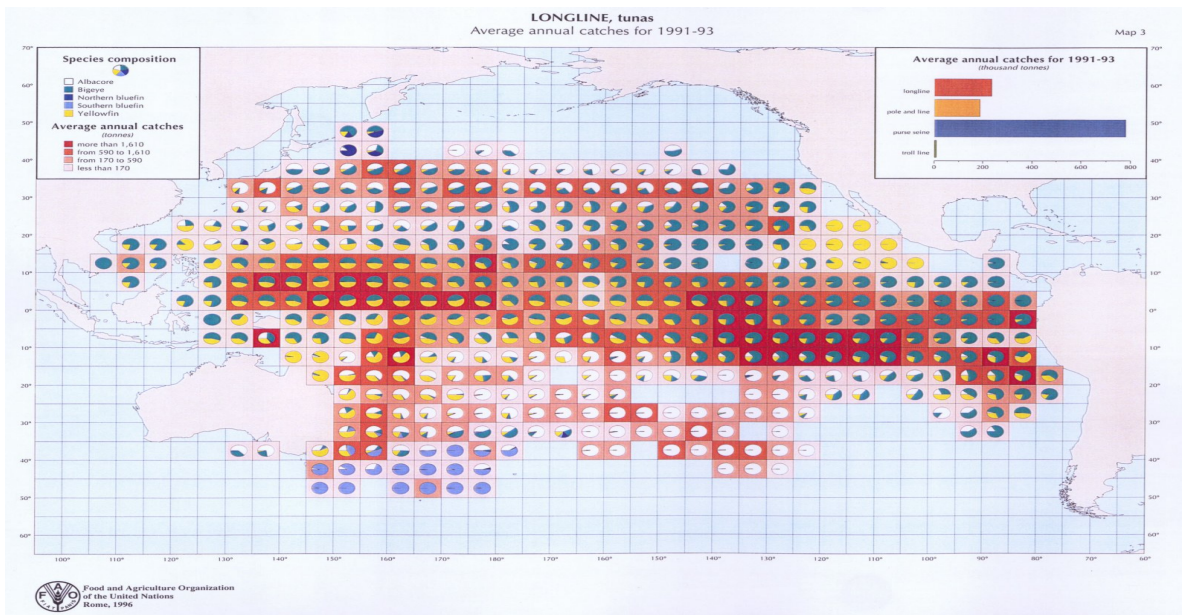


Fig. 1 Averaged annual catch of tuna by longline fishery in 1991-1993 (from UN/FAO publication)

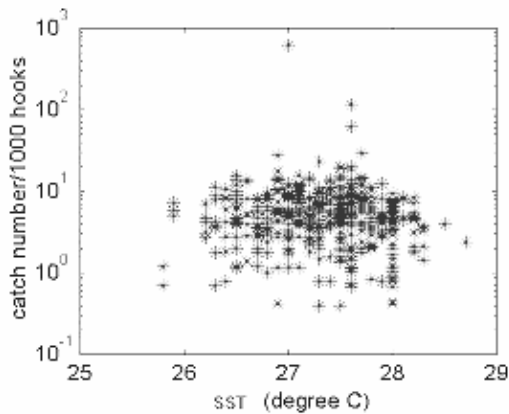


Fig. 2a Scatter diagram of CPUE (log scale) vs. in situ SST from experimental fishing boats.

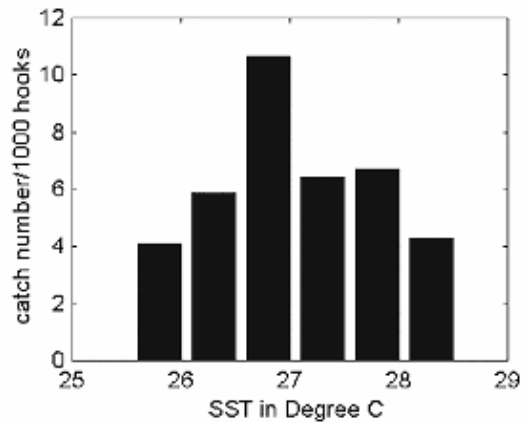


Fig. 2b Bar chart of CPUE (linear scale) vs. in situ SST from experimental fishing boats. CPUE is number of tuna per 1000 hooks

Application of Satellite Remote Sensing on the Tuna Fishery of Eastern Tropical Pacific

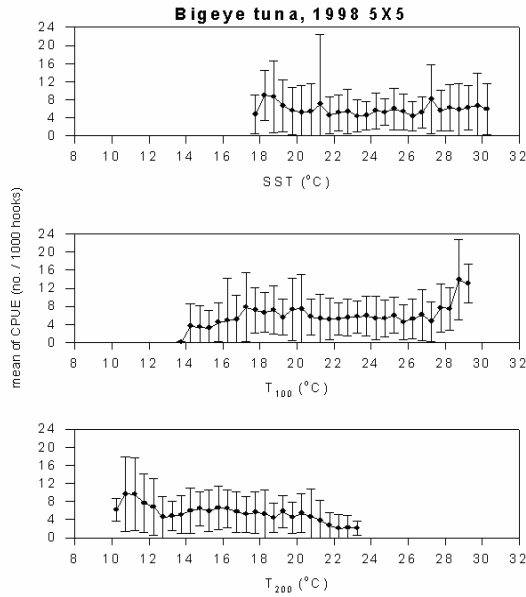


Fig. 3 CPUE of Big Eye tuna vs. monthly mean temperature at surface, 100m and 200 m depth

3 Analysis and Discussion

A direct proof of the fishermen's practice is to compare the CPUE of Big Eye tuna (BET) against the in situ SST that was reported by fishing boats of FA. Figure 2 shows that the CPUE is higher when SST is in the range of 26°C~28°C. How about the CPUE against the mean SST, or the mean water temperature at 100 m and 200 m depth where water temperature changes less than SST and where tuna spends more time during the day.

Figure 3 is a plot of CPUE against the monthly mean water temperature at surface, 100 m and 200 m depth. It is clear that the month mean water temperature does not show much correlation with the CPUE. This is to say that the monthly mean water temperature has little practical value in predicting the fishing ground of BET in ETP.

The reason that figure 2 matches fishermen's experience while figure 3 does not, may be explained by the fast changing marine environmental parameters in ETP, especially near the regions of equatorial upwelling and equatorial fronts between two current systems. To make useful prediction of fishing ground of tuna in ETP, one will need near real-time oceanographic data that are only available through satellite remote sensing.

In most part of the world ocean, satellite-derived SST images of medium to coarse resolution are readily available on the internet. For high resolution satellite-derived SST, it is usually provided by local satellite ground station. Another useful satellite data is the image of ocean color or Chl. a concentration.

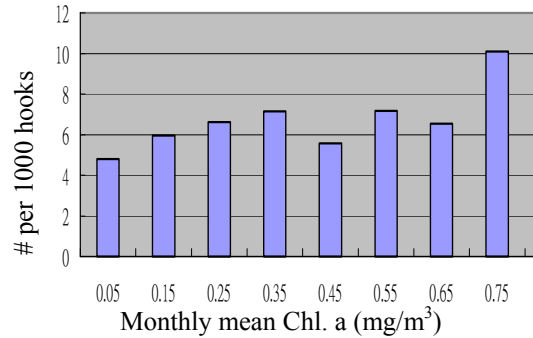


Fig. 4 CPUE of Big Eye tuna vs. monthly mean of satellite-derived Chl. a concentration.

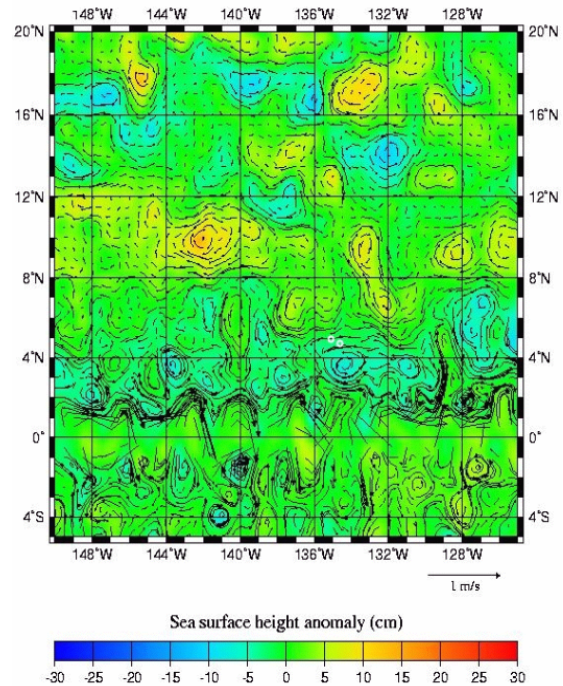


Fig. 5 Eddies and fishing ground: in April of 1999, longline fishing boats (white dots) operated near an eddy centered at (5°N, 135°W)

4 Satellite-Derived Ocean Color

The application of SeaWiFS-derived ocean color images on fishery is well accepted. But in EPT where cloud coverage is high, SeaWiFS sensors can hardly see the sea surface and therefore provide few useful ocean color data. Figure 4 shows the CPUE of BET vs. monthly mean Chlorophyll a (Chl. a) concentration. It is apparent that the correlation is low. But, after comparing the CPUE and satellite-derived Chl. a at the same time and the same location of fishing boat, then we found that CPUE maximizes in regions of moderate productivity, or Chl. a near 0.2 mg/m^3 .

5 Satellite-Derived Ocean Current

In most cases, fishing boats tend to stay away from regions of strong current where deploying fishing gear has more risks. Figure 5 shows that the fishing boat (white dots near $[5^\circ\text{N}, 135^\circ\text{W}]$) tends to work near the edge of eddy and their CPUE of BET is higher for current speed larger than 0.15 m/s (Fig. 6). Again, we did not find this positive correlation between CPUE and the mean current.

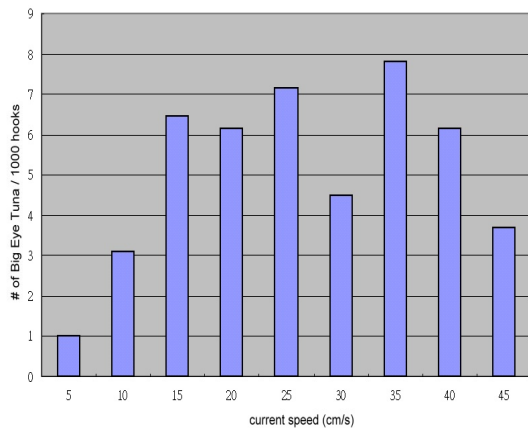


Fig. 6 CPUE of Big Eye tuna vs. the speed of current (cm/s)

6 Satellite-Derived Sea Surface Height (SSH)

The life cycle and the feeding behavior of tuna is still a mystery to us. This mystery is soon to be resolved by the application of Archival Tag.

Figure 7 shows a typical vertical migration of BET in one day. At sunrise, BET dives (blue line in Fig. 7) from surface layer to the dark and cold deep layer (red line in Fig. 7) to hide from predator or to search for food. BET dives to the deepest layer at noon when the sunlight is the highest. But, the deep water is too cold for BET to maintain its body temperature. It has to take many short trips to the upper layer to warm up its body (green line in Fig. 7). The profile of underwater light level varies with solar luminance and water clarity, so the depth that BET hides and hunts also changes with space and time. For the case of Figure 7, if fish hooks were deployed between $0 \sim 80$ meter depth, then BET will not see the hooks at night (no light) or during the day (this BET stays below 80 m). Because most fishhooks are deployed near sea surface (say, around $50\sim 150$ meters), the CPUE depends on the probability that BET will see these hooks. Therefore, the profile of water clarity and water temperature will influence CPUE of BET.

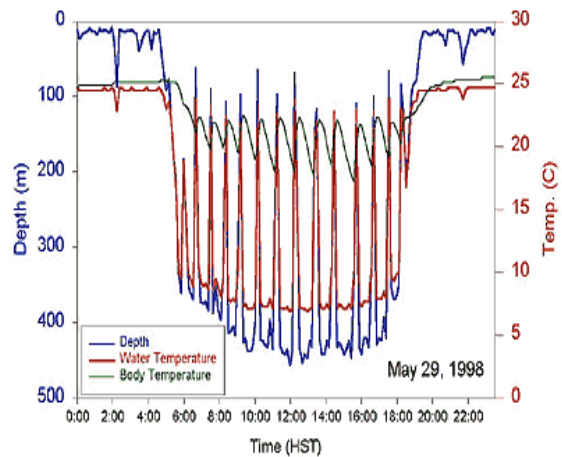


Fig. 7 Vertical daily migration of a Big Eye tuna (source: Archive Tag of NMFS in Hawaii)

Sea surface height (SSH) increases if the vertical integration specific volume is higher. Since water temperature is the major factor in determining SSH, SSH is higher if the vertical mean temperature is higher. In the plot of CPUE of BET vs. SSH, it is clear that CPUE (catch / 1000 hooks) of experimental fishing boats increases with SSH (Fig. 8a). Because the number of deployed hooks is not correlated to the SSH (Fig. 8b), the resulted CPUE should be a non-biased statistic from a non-biased sampling (random sampling) in SSH.

Application of Satellite Remote Sensing on the Tuna Fishery of Eastern Tropical Pacific

A plausible explanation for the dependence of CPUE on SSH is the following: higher SSH is mostly due to thicker surface layer (like a warm eddy) where water is usually more clear, sunlight can penetrate deeper, and BET tends to dive to deeper (and colder) water to hide or to hunt, then BET loses body heat faster in colder water and it has to swim up more frequently, therefore BET has a higher probability to see the hooks (above 150 m depth) and be caught. Therefore, CPUE increases with SST in this region.

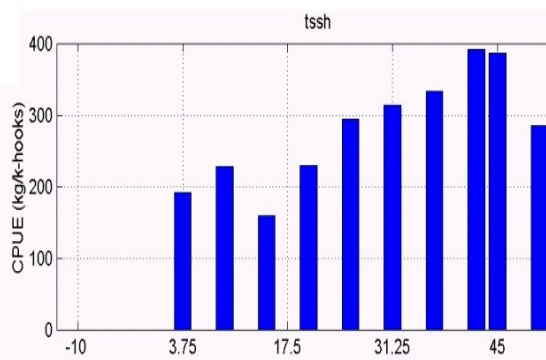


Fig. 8a Mean CPUE vs. sea surface height (cm)

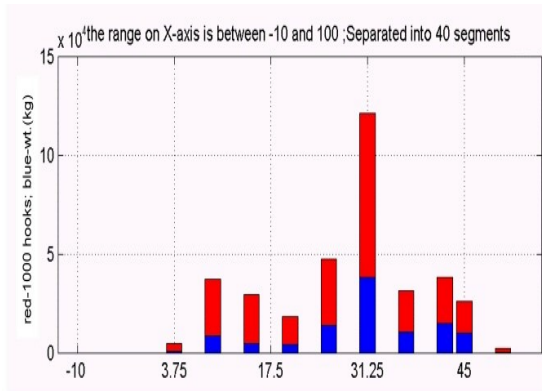


Fig. 8b CPUE of Big Eye tuna (blue) and number of hooks deployed (red) vs. sea surface height (cm)

To further exemplify the dependence of CPUE on SSH (Fig. 8) and the location of eddy (Fig. 5), daily catch of tuna by a fishing boat is plotted (Fig. 9)

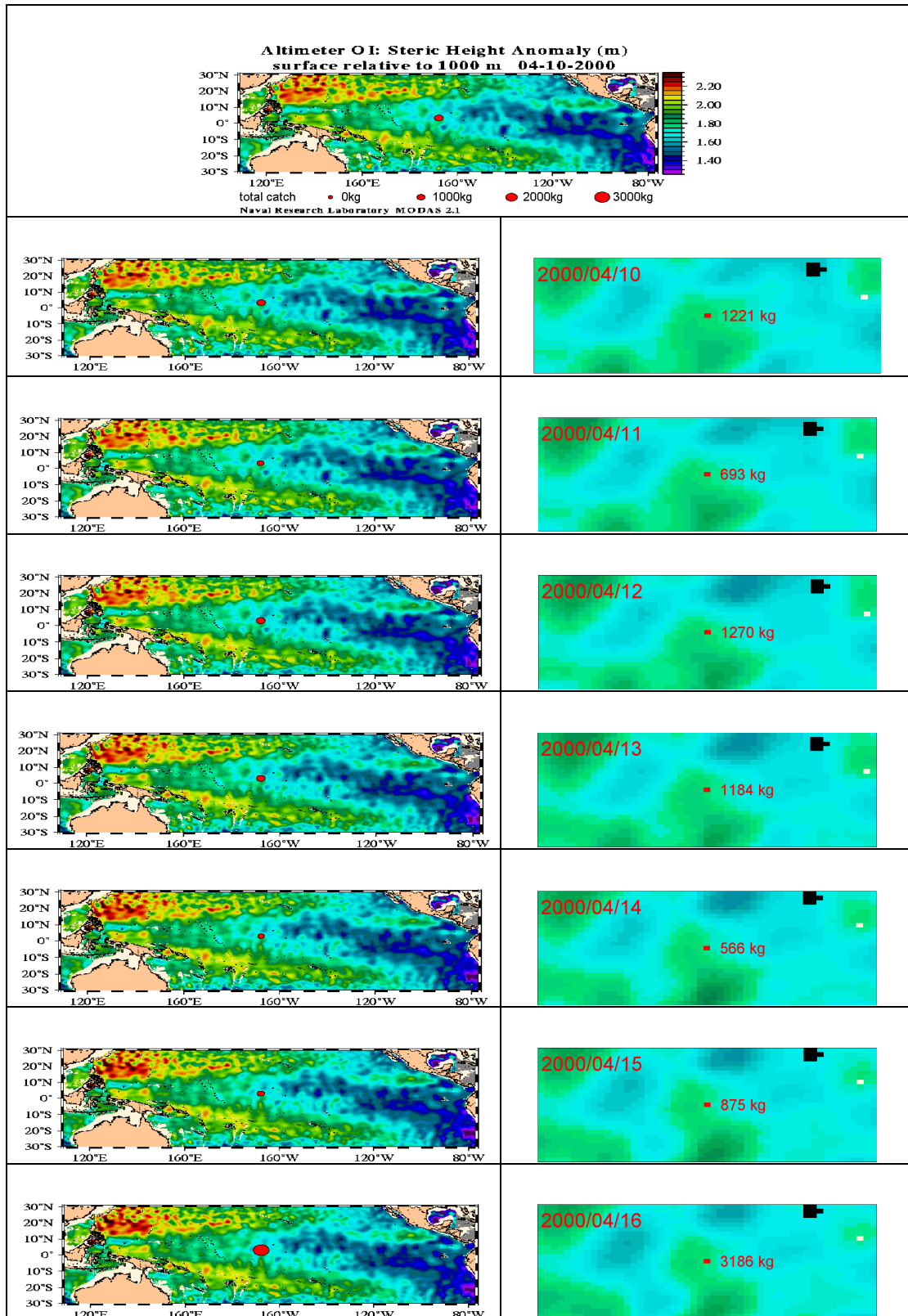
against the daily SSH anomaly (relative to 1000 m depth) that is provided by the Naval Research Laboratory as MODAS 2.1.

Fig. 9 shows daily MODAS SSH images that are overlaid with the daily tuna catch of an experimental fishing boat. The top panel shows the color scale of SSH (1.4 ~ 2.2 m) and red ellipses for total tuna catch of the day. The right panels show the total tuna catches vs. SSHs that were extracted from the left panels. From April 10 to 19, the boat stayed near the edge of an eddy of relatively high SSH, even when the eddy split into two and drifted apart. The total tuna catch stayed high until the eddy faded away on April 20.

7 Conclusion

From above analysis, it is clear that (1) sea surface temperature, ocean color, ocean current and sea surface height are all correlated to the CPUE of Big Eye tuna; (2) these marine environmental parameters are necessary conditions for the prediction of fishing ground of ETP tuna, but none of them is sufficient condition; therefore, one has to weight their contributions in making prediction of fishing ground; (3) The CPUE has little correlation with the long-term mean or large-area averaged oceanographic data; (4) satellite remote sensing can provide the near real-time observation of world ocean that is required for predicting a fast-change fishing ground. Because satellite data have been integrated into the fishing ground prediction by commercial companies, one should be able to do the same if sufficient manpower and time were invested.

Acknowledgement. This study was sponsored by the Fishery Administration of ROC on Taiwan through grants 90AS-1.4.5-FA-F2 and 91AS-2.5.2-FA-F1. We are grateful to Colorado Center for Astrodynamics Research, Naval Research Laboratory, NODC and NASA SeaWiFS Team and NMFS at Hawaii. This study will not be possible without their freely accessible data and figures.



Application of Satellite Remote Sensing on the Tuna Fishery of Eastern Tropical Pacific

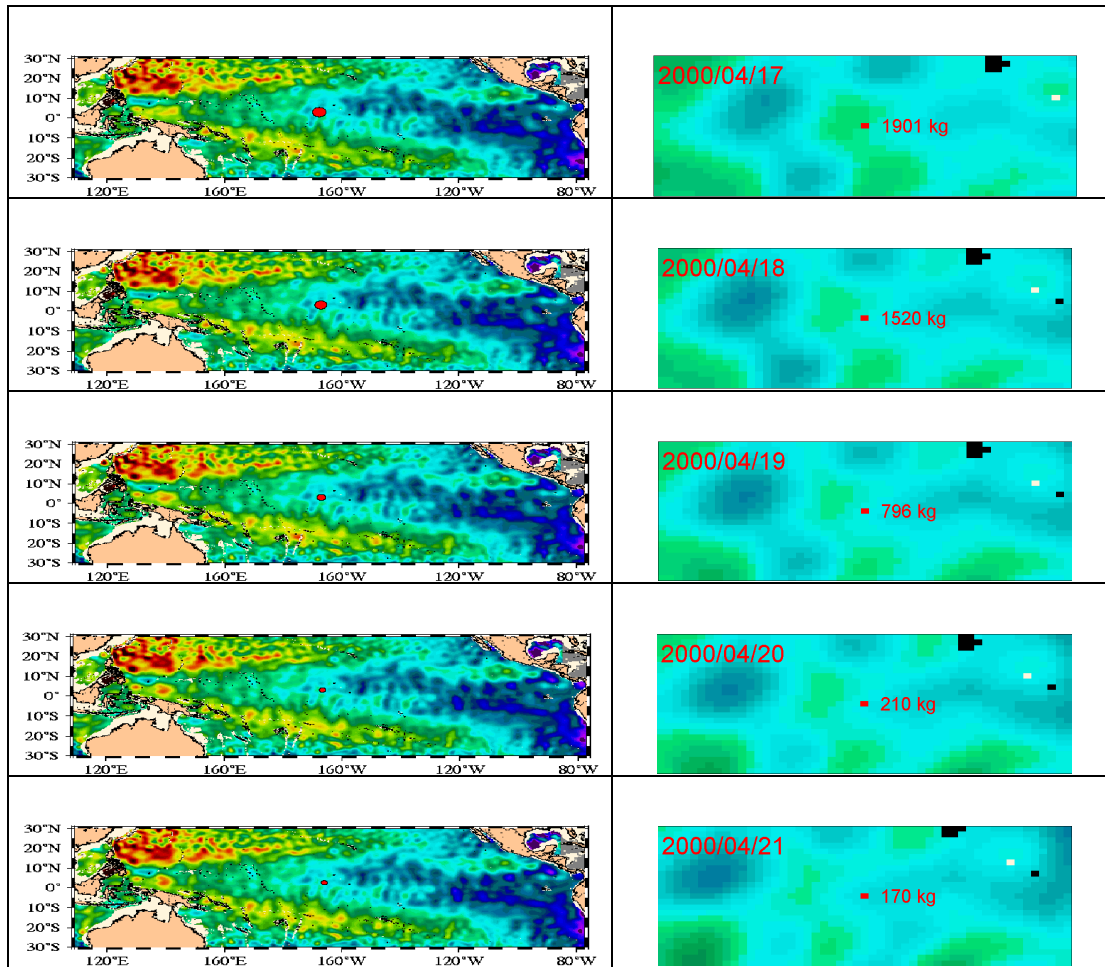


Fig. 9 Total daily catch of tuna is plotted against the sea surface height (SSH) (from MODAS 2.1 by Naval Research Laboratory). Top panel: total catch of tuna on 2000/4/10 vs. SSH (in meters, with color scale on the right). Left panels: daily total tuna catch (red dot with scale in the top panel) vs. SSH. Right panels: daily total tuna catch vs. changing eddy fields. Total tuna catch is high when the boat is near the edge of an eddy of high SSH (green vs. blue-green background), and it is low when the boat is far from eddies. The size of the image covers about 570 km by 1920 km. The tuna catch data were provided by the Fishery Administration of ROC.

Reference

- Baker, K. S., and R. C. Smith (1982). Bio-Optical Classification and Model of Nature Waters, *Limnol Oceanogr*, 27, pp. 500-509.
- Digby, S., T. Antczak, R. Leben, G. Born, S. Barth, R. Cheney, D. Foley, C. Goni, G. Jacobs and N. Shay (1999). Altimeter Data for Operational Use in the Marine Environment, IEEE/MTS Conference "Oceans '99", Seattle, Sept.
- Fu, L. L., and R. E. Cheney (1995). Application of Satellite Altimetry to Ocean Circulation Studies, 1987-1994, *Rev Geophys*, 33, pp. 212-223.
- Gordon, H. R., O. B. Brown, R. H. Evans, J. W. Brown, R. C. Smith, K. S. Baker and D. K. Clark (1988). A Semi-Analytic Radiance Model of Ocean Color, *J Geophys Res*, 93, pp. 10909-10924.
- Ho, C. R., X. H. Yan and Q. Zheng (1995). Satellite Observation of Upper Layer Variabilities in the Western Pacific Warm Pool, *Bull Am Meth Soc*, 76, pp. 669-679.
- Long, B., and P. Chang (1990). Propagation of an Equatorial Kelvin wave in a Varying Thermocline, *J Phys Oceanogr*, 20, pp. 1826-1841.
- Robinson, I. S. (1983). Satellite Observations of Ocean Colour, *Phil. Trans. Roy. Soc. London*, A309, pp. 415-432.
- Wyrki, K. (1987). Indices of Equatorial Currents in the Central Pacific, *Trop Ocean-Atmos Newsletter*, 58, pp. 3-5.
- Wyrki, K., E. Firing, D. Halpern, R. Knox, G. J. McNally, W. C. Patzer, E. D. Stroup, B. A. Taft and R. Williams (1981). The Hawaii to Tahiti Shuttle Experiment, *Science*, 211, pp. 22-28.
- Yan, X. H., Y. He, T. Liu, Q. Zheng and C. R. Ho (1997). Centroid Motion of the Western Pacific Warm Pool in the Three Recent El Nino -- Southern Oscillation Events, *J Phys Oceanogr*, 27, pp. 837-845.
- Yan, X. H., C. R. Ho, Q. Zheng and V. Klemas (1992). Temperature and Size Variabilities of the Western Pacific Warm Pool, *Science*, 258, pp. 1643-1645.

Cho-Teng Liu et. al.

Zheng, Q., X. H. Yan, C. R. Ho and C. K. Tai (1995).
Observation of Equatorially Trapped Waves in the Pacific
Using Geosat Altimeter Data, *Deep-Sea Res*, 42, pp. 797-817.